Chemical Physics Letters 485 (2010) 363–366

Contents lists available at ScienceDirect

Chemical Physics Letters

journal homepage: www.elsevier.com/locate/cplett

Epitaxial $Zn_{1-x}Mg_xO$ films grown on (1 1 1) Si by pulsed laser deposition

X.H. Pan [a,b], W. Guo [b], Z.Z. Ye [a], B. Liu [c], Y. Che [c], C.T. Nelson [b], Y. Zhang [b], W. Tian [d], D.G. Schlom [d], X.Q. Pan [b,*]

[a] State Key Laboratory of Silicon Materials, Zhejiang University, Hangzhou 310027, People's Republic of China
[b] Department of Materials Science and Engineering, University of Michigan, Ann Arbor, MI 48109-2136, USA
[c] Functional Materials Group, IMRA America, Inc., Ann Arbor, MI 48105, USA
[d] Department of Materials Science and Engineering, Cornell University, Ithaca, NY 14853-1501, USA

ARTICLE INFO

Article history:
Received 31 August 2009
In final form 15 December 2009
Available online 21 December 2009

ABSTRACT

$Zn_{1-x}Mg_xO$ thin films are epitaxially grown on (1 1 1) Si substrates using intervening epitaxial Lu_2O_3 buffer layers by pulsed laser deposition. Lu_2O_3 buffer layer on Si substrate is essential to the $Zn_{1-x}Mg_xO$ epitaxial growth. X-ray diffraction, transmission electron microscopy, atomic force microscopy and photoluminescence measurements reveal that the $Zn_{1-x}Mg_xO$ films have high quality structural and optical properties. The films with thickness of 650 nm have a resistivity of 4.18 Ω cm, a Hall mobility of 16.97 $cm^2\ V^{-1}\ s^{-1}$, and an electron concentration of $8.80 \times 10^{16}\ cm^{-3}$ at room temperature.

© 2009 Published by Elsevier B.V.

1. Introduction

ZnO is attracting worldwide attention for potential applications in short-wavelength optoelectronic devices [1,2]. One of the important capabilities involved in constructing optical and electrical confinement structures is band gap engineering. The ternary alloy semiconductor, $Zn_{1-x}Mg_xO$, is considered to have larger fundamental band gap energy than ZnO, and the ability to grow high quality epitaxial $Zn_{1-x}Mg_xO$ thin films may thus be very useful.

Until now, most studies have employed sapphire as the substrate for the growth of $Zn_{1-x}Mg_xO$ [3–6]. However, sapphire, an electrically insulating material, has obvious limitations with respect to device fabrication and future optoelectronic integration for industrial application. It is clearly useful to be able to grow $Zn_{1-x}Mg_xO$ films on a semiconductor material, such as Si, because manufacturing of Si-based devices has been well developed. However, the direct growth of $Zn_{1-x}Mg_xO$ on Si has been recognized as a difficult task because of the easy oxidation of the Si surface and the large mismatches in lattice (15.4%) and thermal expansion coefficient (60%) between $Zn_{1-x}Mg_xO$ and Si [7]. In addition, investigations of epitaxial $Zn_{1-x}Mg_xO$ films grown on Si are limited [8,9]. Thus, more effort should be directed toward the growth of $Zn_{1-x}Mg_xO$ films on Si. Instead, intervening buffer layers may be used in order to improve the crystal quality of $Zn_{1-x}Mg_xO$ films grown on Si. Based on previous study on epitaxial ZnO films grown on Si [10–14], intervening epitaxial Lu_2O_3 buffer layer is one of the best buffer layers [14]. This method is also used to grow $Zn_{1-x}Mg_xO$ films. In this work, we investigate $Zn_{1-x}Mg_xO$ thin films grown on Si using intervening epitaxial Lu_2O_3 buffer layers.

2. Experiments

Epitaxial Lu_2O_3 buffer layers with a thickness of 30 nm are grown on *n*-type (1 1 1) Si wafers by reactive molecular beam epitaxy (MBE). Prior to growth, the native SiO_2 on the Si wafers is removed by HF dipping. Once the SiO_2 is removed, the Si wafers are immediately placed into the MBE chamber in which the typical base pressure is $\sim 5 \times 10^{-10}$ Torr. The Lu_2O_3 buffer layers are grown using elemental Lu source. During growth, the substrates are held at 700 °C measured by an optical pyrometer and immersed in a continuous flux of molecular oxygen, yielding a O_2 partial pressure of 2×10^{-6} Torr. Detailed growth conditions are given in [15].

The $Zn_{1-x}Mg_xO$ films are grown on (1 1 1) Lu_2O_3/(1 1 1) Si substrates by pulsed laser deposition using a target of high purity ZnO–MgO ceramic disk with Mg content of 10 at.%. Henceforth, the $Zn_{1-x}Mg_xO$ thin films grown using this target will be referred to as $Zn_{0.9}Mg_{0.1}O$. A KrF excimer laser (λ = 248 nm) is employed to ablate the target. The films are grown in two steps. First, a 10-nm-thick $Zn_{0.9}Mg_{0.1}O$ layer is grown at low substrate temperature (240 °C), which enhances nucleation of the $Zn_{0.9}Mg_{0.1}O$ film. Then, the remainder of the $Zn_{0.9}Mg_{0.1}O$ film is deposited at 600 °C in an oxygen ambient of 5.0×10^{-3} Torr. The structural, optical and electrical properties of the $Zn_{0.9}Mg_{0.1}O$ films are investigated by X-ray diffraction (XRD), transmission electron microscopy (TEM), atomic force microscopy (AFM), temperature-dependent photoluminescence (PL), and Hall measurements. The PL spectra are measured using a 100 mW He–Cd laser (λ = 325 nm) as the excitation source and a HORIBA Jobin-Yvon 1 m monochromator.

3. Results and discussion

Fig. 1a shows a $\theta - 2\theta$ XRD pattern, typical of all $Zn_{0.9}Mg_{0.1}O$ samples grown on (1 1 1) Lu_2O_3/(1 1 1) Si substrates. The

* Corresponding author. Fax: +1 734 763 4788.
E-mail address: panx@umich.edu (X.Q. Pan).

0009-2614/$ - see front matter © 2009 Published by Elsevier B.V.
doi:10.1016/j.cplett.2009.12.046

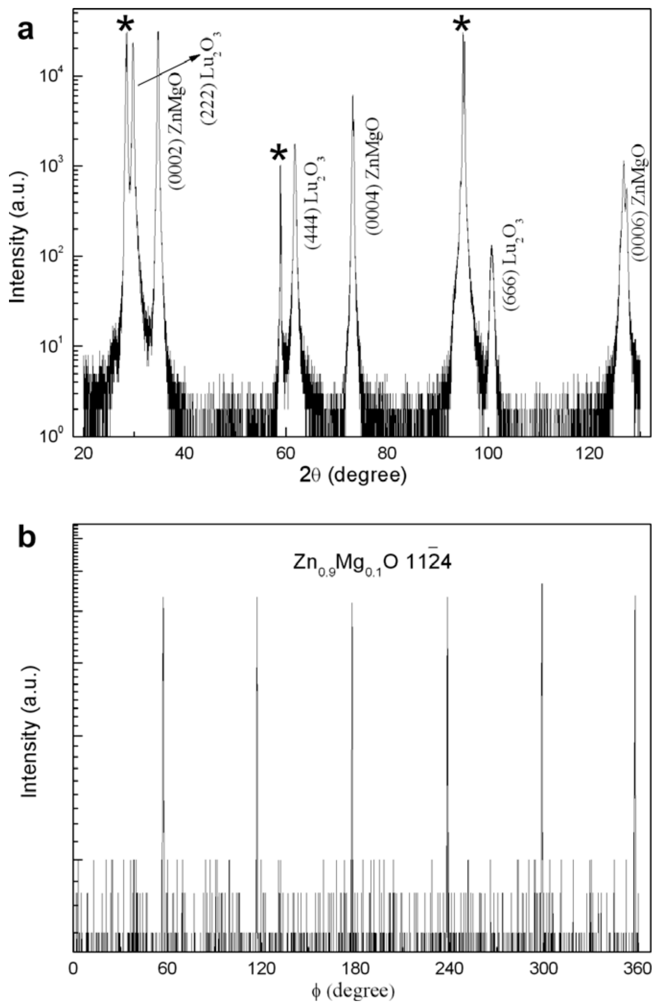

Fig. 1. (a) Typical $\theta - 2\theta$ XRD pattern of a $Zn_{0.9}Mg_{0.1}O$ thin film grown on (1 1 1) Lu_2O_3/(1 1 1) Si. '*' Denotes peaks due to the (1 1 1) Si substrates. (b) $1 1 \bar{2} 4$ ϕ-scan of the same $Zn_{0.9}Mg_{0.1}O$ film.

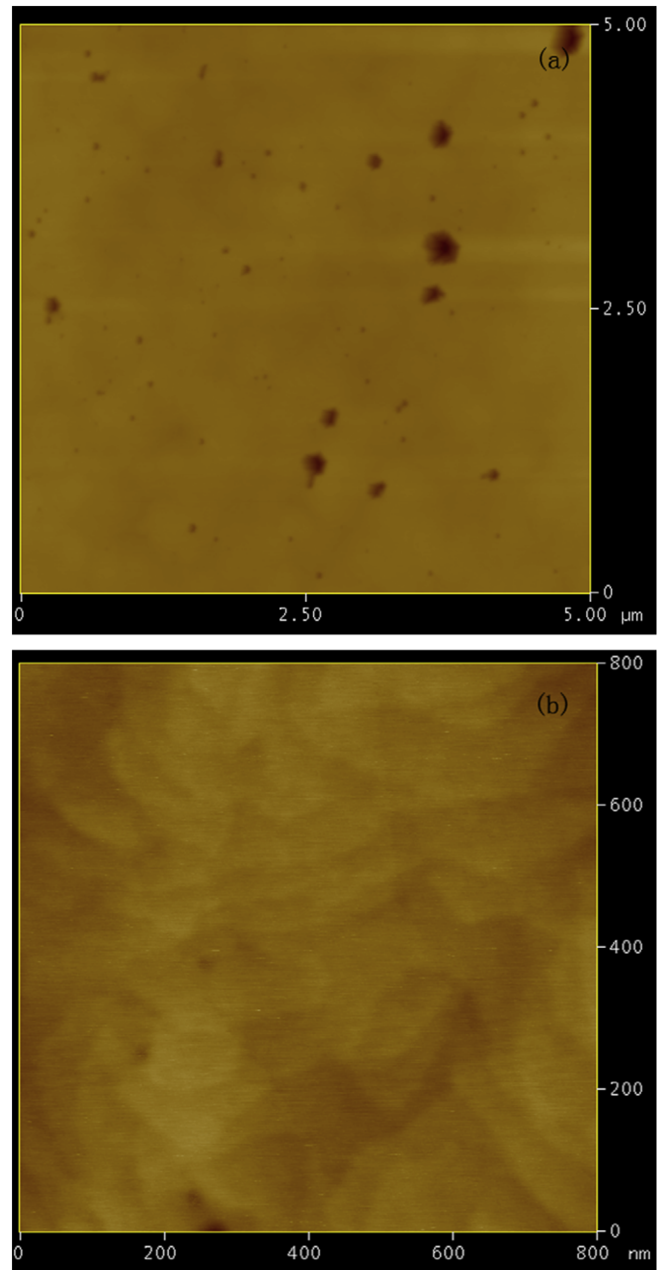

Fig. 2. AFM images of $Zn_{0.9}Mg_{0.1}O$ film grown on (1 1 1) Lu_2O_3/(1 1 1) Si from a scale of: (a) 5 × 5 μm and (b) 0.8 × 0.8 μm.

out-of-plane orientation relationship is $(0\,0\,0\,1)_{ZnO} \,\|(1\,1\,1)_{Lu_2O_3}\|$ $(1\,1\,1)_{Si}$. Only peaks corresponding to $Zn_{0.9}Mg_{0.1}O$ (0 0 0 2), (0 0 0 4) and (0 0 0 6) planes are observed, and no extra $Zn_{0.9}$-$Mg_{0.1}O$ or impurity peaks are detected. The ϕ-scan of the $1 1 \bar{2} 4$ reflection of $Zn_{0.9}Mg_{0.1}O$ shown in Fig. 1b clearly indicates the six-fold symmetry of $Zn_{0.9}Mg_{0.1}O$, which means that the $Zn_{0.9}Mg_{0.1}O$ films are epitaxially grown on (1 1 1) Lu_2O_3/(1 1 1) Si. The full-width at half-maximum (FWHM) values of the 0 0 0 2 and $1 0 \bar{1} 2$ $Zn_{0.9}Mg_{0.1}O$ ω-rocking curves are 0.193° and 0.287° for a 650 nm thick $Zn_{0.9}Mg_{0.1}O$ film. These values are reasonable, considering the degradation of the film crystallinity caused by alloying Mg in ZnO. Using the angle position of (2 2 2) peak of Si as reference, the angle position of (0 0 0 2) peak (θ value) changes from 17.2105° of pure ZnO to 17.3385° of $Zn_{0.9}Mg_{0.1}O$ (data not shown). According to this value, the *c*-axis lattice parameter is determined to be 5.1695 Å, which is smaller than 5.2069 Å of bulk ZnO.

The surface morphology of a typical $Zn_{0.9}Mg_{0.1}O$ film is shown in the AFM images of Fig. 2. From Fig. 2a, the root mean square (rms) surface roughness (determined on an area of 5 × 5 μm) of the $Zn_{0.9}Mg_{0.1}O$ film is about 1.813 nm. Fig. 2b shows a smaller area (0.8 × 0.8 μm) from the same film, in which the rms roughness is much less, only 0.221 nm.

Fig. 3a shows a cross-sectional TEM image of a $Zn_{0.9}Mg_{0.1}O$ film grown on (1 1 1) Lu_2O_3/(1 1 1) Si substrate. It is apparent that both the $Zn_{0.9}Mg_{0.1}O$ film and Lu_2O_3 buffer layer have uniform thickness and smooth interfaces. A few threading dislocations originate from the $Zn_{0.9}Mg_{0.1}O/Lu_2O_3$ interface and propagate through the film. The high-resolution TEM (HRTEM) image in Fig. 3b reveals an atomically sharp interface between the $Zn_{0.9}Mg_{0.1}O$ and Lu_2O_3 layers. Although not shown, the Lu_2O_3/Si interface is also atomically sharp without any amorphous layer, as determined by the HRTEM study.

Hall measurements, performed at room temperature, of a 650 nm thick film of $Zn_{0.9}Mg_{0.1}O$ found a resistivity of 4.18 Ω cm, a Hall mobility of 16.97 $cm^2\,V^{-1}\,s^{-1}$, and an electron concentration of $8.80 \times 10^{16}\,cm^{-3}$. Compared with the Hall data of epitaxial ZnO films on (1 1 1) Lu_2O_3/(1 1 1) Si substrates [14], the $Zn_{0.9}Mg_{0.1}O$ films thus generally show higher resistivity, lower mobility, and lower electron concentration, as shown in Table 1. Our explanation for this is as follows: First, alloying Mg in ZnO will increase the band gap of ZnO, shift the conduction-band edge to higher energy,

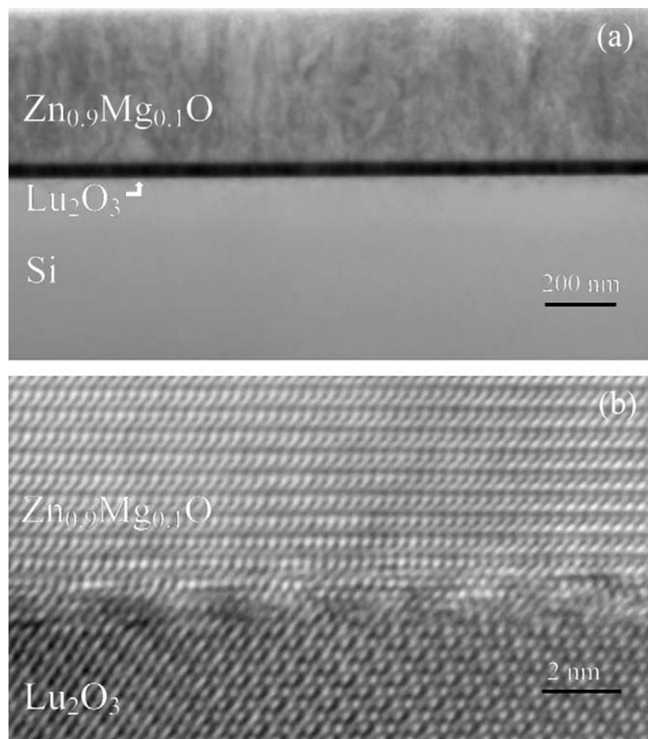

Fig. 3. (a) Cross-sectional TEM image of a $Zn_{0.9}Mg_{0.1}O$ film grown on (1 1 1) Lu_2O_3/(1 1 1) Si substrate. (b) High-resolution TEM image of the $Zn_{0.9}Mg_{0.1}O/Lu_2O_3$ interface.

Table 1
Electrical properties of epitaxial $Zn_{0.9}Mg_{0.1}O$ and ZnO thin films on (1 1 1) Lu_2O_3/(1 1 1) Si substrates.

Sample	Resistivity (Ω cm)	Hall mobility ($cm^2 V^{-1} s^{-1}$)	Electron concentration (cm^{-3})
$Zn_{0.9}Mg_{0.1}O$	4.18	16.97	8.80×10^{16}
ZnO	0.31	80	2.5×10^{17}

and increase the activation energy of the defect donor states, which lead to a decrease of the n-type background carrier concentration and an increase of the resistivity. Second, a high Mg concentration added in ZnO will induce a larger population of structural distortion, which consequently results in a decrease of the mobility.

Fig. 4a shows the 10 K PL spectrum of $Zn_{0.9}Mg_{0.1}O$ films. In the spectrum, four peaks can be distinguished in linear scale (inset of Fig. 4a), while even more peaks can be observed in logarithmic scale. This indicates the $Zn_{0.9}Mg_{0.1}O$ films grown on (1 1 1) Lu_2O_3/(1 1 1) Si have good optical properties. In addition, all the PL peaks show a blueshift compared with those of pure ZnO film, which confirms that alloying Mg in ZnO increases the fundamental band gap energy of ZnO. The strongest PL peaks, labeled as X and Y, at 3.558 and 3.578 eV, are assigned to neutral donor bound exciton (D^0X) and ionized donor bound exciton transitions (D^+X). On the high-energy side of Y, a shoulder labeled as Z, at 3.593 eV, is identified as the ground state emission of A free exciton (FX_A). On the low-energy side of X, the first two peaks (near X) are assigned to FX longitudinal optical (LO) phonon replicas, and assignments of other two peaks are in progress.

To support our assignments, temperature-dependent PL spectra are also shown in Fig. 4a. At low temperature (10 K), the spectra are dominated by peak X. As the temperature increases, peak X shows a redshift and gradually quenches, to the benefit of peak Z. Fig. 4b plots the intensity of peak X as a function of reciprocal temperature. The data can be described by the expression [16]

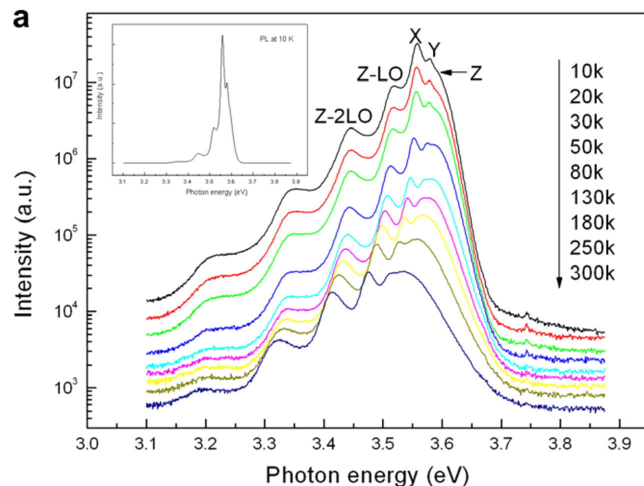

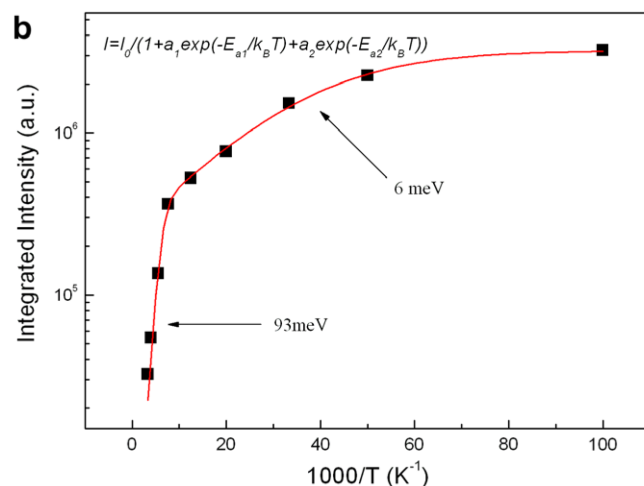

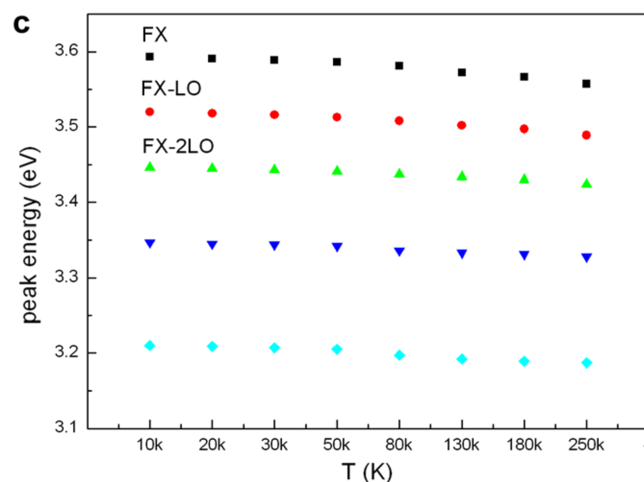

Fig. 4. (a) Temperature-dependent PL spectra of NBE emissions of the same film studied in Fig. 1. The inset shows the PL spectrum at 10 K in linear scale. (b) Integrated intensity of X emission in (a) as a function of reciprocal temperature. (c) Temperature-dependent peak positions of peak Z and other four peaks.

$$I = I_0/[1 + a_1 \exp(-E_{a_1}/kT) + a_2 \exp(-E_{a_2}/kT)], \quad (1)$$

where E_a is the activation energy for the thermal quenching process and k is the Boltzmann constant. In this expression, the presence of two E_a indicates two competitive nonradiative recombination channels. The curve fitting gives rise to two activation energies of about

6 and 93 meV. The 6 meV activation energy is much smaller than the localization energy of ZnO. Krustok et al. [17] have pointed out that such a low E_a value of a few meV may just result from the temperature-dependent capture cross section of the carriers at the recombination centers, but not from a genuine thermal activation energy. Considering alloying Mg in ZnO increases the fundamental band gap energy of ZnO, it is reasonable to infer that the addition of Mg may shift the conduction-band edge to higher energy, and increase the activation energy of the donor states. The quenching is, therefore, attributed to the thermal ionization of D^0X with an activation energy of 93 meV. Based on the above analysis, PL peak X, at 3.558 eV, is believed to D^0X.

The temperature-dependent band gap is described as

$$E_g(T) = E_g(0) - \alpha T^2/(T + \beta), \tag{2}$$

according to [18], where $E_g(T)$ is the temperature-dependent band gap energy, α and β are constant, and T is the temperature. The energy of peak Z fits well a curve of $E_g(T)$ – 60 meV (data not shown), confirming it has typical FX characteristics.

The temperature dependence of the other four peak positions is shown in Fig. 4c. The first two peaks have an energy separation of approximately 70 meV, which is close to the LO phonon energy found in pure ZnO thin film [19]. At the present Mg concentration of 10 at.%, the LO phonon energy is nearly the same as in pure ZnO thin film [20]. Also, the temperature dependence of the peaks is nearly the same as FX, so the first two peaks are identified as FX-LO phonon replicas. For other two peaks, the temperature dependence is similar to FX, but with an energy separation larger than 70 meV. The origin of the larger separation is not fully understood now, but it could be related to the addition of Mg in ZnO. Further study of their assignment is in progress.

4. Conclusions

In conclusion, we have fabricated epitaxial $Zn_{0.9}Mg_{0.1}O$ thin films on Si substrates by pulsed laser deposition using intervening epitaxial Lu_2O_3 buffer layers. Good structural, optical and electrical qualities are revealed from XRD, AFM, TEM, temperature-dependent PL and Hall studies. It is likely that the epitaxial growth of $Zn_{0.9}Mg_{0.1}O$ films on Si will see significant progress in the near future and contribute to the integration of ZnO-based ultraviolet optoelectronic devices with Si electronics.

Acknowledgments

This work was mainly supported by the US National Science Foundation under grants NSF/DMR 0308012 and 0907191. Partial supports were from the National Basic Research Program of China (Grant No. 2006CB604906), the Natural Science Foundation of China (Grant No. 50532060), and Intel.

Appendix A. Supplementary material

Supplementary data associated with this article can be found, in the online version, at doi:10.1016/j.cplett.2009.12.046.

References

[1] Z.K. Tang, G.K.L. Wong, P. Yu, M. Kawasaki, A. Ohtomo, H. Koinuma, Y. Segawa, Appl. Phys. Lett. 72 (1998) 3270.
[2] D.C. Look, Mater. Sci. Eng. B 80 (2001) 383.
[3] A. Ohtomo et al., Appl. Phys. Lett. 72 (1998) 2466.
[4] A.K. Sharma et al., Appl. Phys. Lett. 75 (1999) 3327.
[5] S. Choopun, R.D. Vispute, W. Yang, R.P. Sharma, T. Venkatesan, H. Shen, Appl. Phys. Lett. 80 (2002) 1529.
[6] S. Heitsch et al., J. Appl. Phys. 101 (2007) 083521.
[7] K. Iwata et al., J. Cryst. Growth 214 (2000) 50.
[8] M. Fujita, M. Sasajima, Y. Deesirapipat, Y. Horikoshi, J. Cryst. Growth 278 (2005) 293.
[9] K. Koike et al., J. Cryst. Growth 278 (2005) 288.
[10] A. Nahhas, H.K. Kim, J. Blachere, Appl. Phys. Lett. 78 (2001) 1511.
[11] K. Koike, T. Komuro, K. Ogata, S. Sasa, M. Inoue, M. Yano, Phys. E 21 (2004) 679.
[12] L. Wang et al., J. Cryst. Growth 284 (2005) 459.
[13] X.N. Wang et al., Appl. Phys. Lett. 90 (2007) 151912.
[14] W. Guo, A. Allenic, Y.B. Chen, X.Q. Pan, W. Tian, C. Adamo, D.G. Schlom, Appl. Phys. Lett. 92 (2008) 072101.
[15] W. Tian, L.F. Edge, D.G. Schlom, D.O. Klenov, S. Stemmer, V.V. Afanas'ev, A. Stesmans, unpublished.
[16] M. Leroux, N. Grandjean, B. Beaumont, G. Nataf, F. Semond, J. Massies, P. Gibart, J. Appl. Phys. 86 (1999) 3721.
[17] J. Krustok, H. Collan, K. Hjelt, J. Appl. Phys. 81 (1997) 1442.
[18] L.J. Wang, N.C. Giles, J. Appl. Phys. 94 (2003) 973.
[19] N. Ashkenov et al., J. Appl. Phys. 93 (2003) 126.
[20] C. Bundesmann et al., Appl. Phys. Lett. 81 (2002) 2376.